# Surface $pCO_2$ and hydrography in the dense water formation area of the southern Adriatic

Carlotta Dentico[1,2], Angelo Rubino[1], Giuseppe Civitarese[2], Michele Giani[2], Giuseppe Siena[2], Stefano Kuchler[2], Julien Le Meur[2], Andrea Corbo[2] and Vanessa Cardin[2]

[1] Department of Environmental Sciences, Informatics and Statistics, Università Cà Foscari, Venice, Italy
[2] National Institute of Oceanography and Applied Geophysics (OGS), Trieste, Italy

Correspondence to: Carlotta Dentico (cdentico@ogs.it)

**Abstract.**

The rising $CO_2$ concentration in the atmosphere leads to an increase in $CO_2$ uptake by the ocean and to significant changes in seawater chemistry. These changes, in turn, exert profound effects on marine ecosystems across multiple trophic levels. The Mediterranean Sea is considered a hotspot for climate change. Despite such relevance, observations and studies on its carbonate system remain limited, especially in regions that play a crucial role in regulating air-sea $CO_2$ exchange such as intermediate and dense water formation areas. The southern Adriatic Sea, a key site for dense water formation in the eastern Mediterranean, hosts the EMSO ERIC and ICOS ERIC South Adriatic observatory (EMSO-E2M3A), operated by the Italian National Institute of Oceanography and Applied Geophysics (OGS). This facility allows the study of physical and biogeochemical dynamics in the deepest area of the Adriatic Sea. The suite of sensors deployed on the surface buoy allows for the characterization of water mass properties, biogeochemical cycles, dense water formation process, and ocean acidification, particularly in relation to carbon sequestration dynamics. Here, time series of meteorological data (e.g., wind speed, wind direction), sea surface physical parameters (e.g., temperature, salinity), dissolved oxygen and partial pressure of $CO_2$ ($pCO_{2sw}$) and pH from 2014 to 2024 will be presented (https://doi.org/10.13120/y2hw-1j63, Cardin et al., 2025b). In particular, quality check, correction and post-processing methods applied to the data will be discussed. The validated surface dataset provides a consistent $pCO_{2sw}$ time series for the Adriatic Sea, with values and seasonal variability in agreement with previous observations across the Mediterranean. Associated temperature, salinity, oxygen, and wind measurements reproduce expected regional patterns, confirming the robustness and suitability of the presented dataset for further biogeochemical and climate-related analyses.

## 1. Introduction

The concentration of $CO_2$ in the atmosphere has rapidly increased from around 280 parts per million (ppm) at the beginning of the Industrial Revolution in 1750, to 427 ppm in February 2025 (http://co2.earth/). This increase is the primary driver of the intensification of the ocean $CO_2$ sink, which has increased from $1.2 \pm 0.4$ GtC $yr^{-1}$ in the 1960s to $2.9 \pm 0.4$ GtC $yr^{-1}$ in the period 2014 - 2023 (Friedlingstein et al., 2025). However, the net air-sea $CO_2$ flux is a highly dynamic process exhibiting significant spatial and temporal heterogeneity driven by complex natural and anthropogenic processes (Takahashi et al., 2009; Friedlingstein et al., 2025).

**ha formattato:** Colore carattere: Rosso, Inglese (Regno Unito)

**ha formattato:** Colore carattere: Rosso, Inglese (Regno Unito)

**ha formattato:** Colore carattere: Rosso, Inglese (Regno Unito)

**ha formattato:** Colore carattere: Rosso, Inglese (Regno Unito)

**ha formattato:** Colore carattere: Rosso, Inglese (Regno Unito), Apice

**ha formattato:** Colore carattere: Rosso, Inglese (Regno Unito)

**ha formattato:** Colore carattere: Rosso, Inglese (Regno Unito), Apice

This accelerated oceanic $CO_2$ uptake is the direct cause of changes in seawater chemistry commonly referred to as ocean acidification (OA). These changes are associated with a reduction in seawater pH and carbonate ion concentrations, and an increase in dissolved $CO_2$, dissolved inorganic carbon and bicarbonate ions (Orr et al., 2015). OA poses a significant threat to marine ecological communities (e.g., Gattuso and Hansson, 2011; Riebesell et al., 2013; IPCC, 2021), which rely on specific ranges of key carbonate chemistry parameters for their survival. Continuous, high-quality ocean carbon data are therefore essential to monitor these changes, predict future impacts, and contribute to the biogeochemical Essential Ocean Variables (EOVs) framework of the Global Ocean Observing System (GOOS).

The Mediterranean Sea is a recognized climate change hotspot (e.g., Zittis et al., 2019; Urdiales-Flores et al., 2023; Lazoglou et al., 2024). The unique hydrological and biogeochemical characteristics of the Mediterranean Sea waters (Alvarez et al., 2023) enhance the uptake and transfer of $CO_2$ to depth more efficiently than the global ocean (Schneider et al., 2010; Hassoun et al., 2015), with anthropogenic $CO_2$ having already penetrated all major water masses of the basin (Touratier and Goyet, 2011; Hassoun et al., 2015; Ingrosso et al., 2017). Research has shown that the Mediterranean Sea is already experiencing negative pH trends (e.g., Hassoun et al., 2015; Kapsenberg et al., 2017; Cantoni et al., 2024; Garcia-Ibanez et al., 2024), often with a wider range than those observed in the Atlantic Ocean. However, reliable biochemical and biological carbonate system data remain limited (Hassoun et al. 2022), and comprehensive OA data are still sparse, not easily accessible and often not scalable. Within the Mediterranean, the southern Adriatic Sea is a particularly critical region, serving as the primary site for dense water formation in the eastern Mediterranean (Robinson et al., 2001). About 82% of the Adriatic Dense Water (AdDW) is formed by winter convection (Ingrosso et al., 2017), while the remaining part has its origin on the northern Adriatic shelf and in the middle Adriatic (Ovchinnikov et al., 1985; Bignami et al., 1990; Malanotte-Rizzoli, 1991). The Northern Adriatic Dense Water (NAdDW) is formed in winter, due to the cooling of the entire water column caused by E-NE wind (named Bora). Winter convection and intense Bora winds produce the densest (potential density anomaly, $\sigma_\theta$ = 29.2 kg $m^{-3}$) water mass in the Mediterranean Sea (Malanotte-Rizzoli, 1991; Artegiani et al., 1997). These meteorological and oceanographic conditions which favour heat loss, can also favour $CO_2$ dissolution when surface water is undersaturated with respect to the overlying atmosphere (Cantoni et al., 2024). The NAdDW is partially collected in the middle Adriatic and partly flows southward to the deepest part of the southern Adriatic, ventilating the deep southern Adriatic Pit (Cardin et al., 2011; Cantoni et al., 2016; Le Meur et al., 2025). Previous studies have demonstrated that NAdDW enriched in $CO_2$ water mass cascades in the southern Adriatic deepest layers and mixes with ambient waters, leading to substantial modifications of the $CO_2$ content of AdDW (Cantoni et al., 2016; Ingrosso et al., 2017). Additionally, Ingrosso et al. (2017) provided the first observational evidence of the role of southern Adriatic dense water formation in the sequestration of anthropogenic $CO_2$, capturing conditions indicative of vertical convection and $CO_2$ accumulation at intermediate depths. These findings highlight the importance of sustained observations for understanding carbon dynamics in this dense water formation region. In this context, the physical and biogeochemical properties of the southern Adriatic Sea (SAd) are monitored through coordinated open-ocean observations, including research vessels, moorings, and autonomous platforms such as ocean gliders and Argo floats. Here, meteorological, physical and biogeochemical data collected by the EMSO ERIC and ICOS ERIC South Adriatic observatory named EMSO-E2M3A, operated by the Italian National Institute of Oceanography and Applied Geophysics (OGS) will be presented. EMSO-E2M3A is part of the European Multidisciplinary

**ha formattato:** Colore carattere: Rosso, Inglese (Regno Unito)

**ha formattato:** Colore carattere: Rosso, Inglese (Regno Unito)

**ha formattato:** Colore carattere: Rosso, Inglese (Regno Unito)

**ha formattato:** Colore carattere: Rosso

**ha formattato:** Colore carattere: Rosso

**ha formattato:** Colore carattere: Rosso

**ha formattato:** Colore carattere: Rosso

**ha formattato:** Colore carattere: Rosso

**ha formattato:** Colore carattere: Rosso

Seafloor and Water Column (EMSO) - South Adriatic Regional Facility - (EMSO ERIC) and of the Integrated Carbon Observation System (ICOS) networks. It has been in operation since 2006 representing the longest open-ocean time series in the whole Adriatic making it an ideal site for the investigations of several physical (Bensi et al., 2013, 2014; Cardin et al., 2020; Amorim et al., 2024; Le Meur et al., 2025) and biogeochemical processes (Ingrosso et al., 2017) in the whole water column, as well as air-sea interactions. The time series presented here represents an important resource to understand physical and biogeochemical changes occurring in the region, the OA and the biological responses of planktonic organisms, and to evaluate biogeochemical model performance. A potential use of this time series will also be discussed, in particular related to the calculation of sea–air $CO_2$ flux and the associated uncertainties. Ultimately, this dataset and its potential applications will contribute to assess the role of the southern Adriatic in regulating $CO_2$ exchange and to quantify the carbon stored in the deep layers.

## 2. Material and methods

### 2.1. Study area

The southern Adriatic (SAd) is the deepest part of the Adriatic Sea, with the southern Adriatic Pit (SAP) reaching maximum depths of approximately 1250 m (Figure 1a). This area is featured by a quasi-permanent cyclonic circulation, and dense water formation takes place at the centre of the gyre through winter open-ocean convection (Ovchinnikov et al., 1985; Gačić et al., 1997) contributing to the eastern Mediterranean thermohaline circulation (Robinson et al., 2001). Different water masses can be distinguished in the SAd: i) the Adriatic Surface Water (AdSW) is a relatively fresh and warm water mass, which originates from the Po River runoff and flows southward along a narrow coastal layer of the western Italian shelf and exits through the Strait of Otranto; ii) the Ionian Surface Water (ISW), entering the basin in the eastern part of the Otranto Strait, can be found in the upper part of the water column; iii) Eastern Intermediate Water (EIW) which is not a water mass per se, but the combination of Levantine Intermediate Water (LIW) and Cretan Intermediate Water (CIW; Schroeder et al., 2024); iv) the Adriatic Deep Water (AdDW), which represents one of the main components of deep waters for the whole Eastern Mediterranean basin (Schlitzer et al., 1991; Roether and Schlitzer, 1991; Schroeder et al., 2024), and occupies the bottom layer of the SAP. The hydrological and biogeochemical dynamics of the SAd are strictly linked to that of the Ionian Sea (IS) by means of the Bimodal Oscillating System (BiOS) that changes the circulation of the North Ionian Gyre (NIG) from cyclonic to anticyclonic and vice versa, on decadal time scale (Gačić et al., 2011; Civitarese et al., 2023). The anticyclonic phase of the NIG leads to the entrance of the Atlantic Water, which decreases the salinity and the density of the AdDW. The cyclonic phase brings warm and salty EIW and Levantine Surface Water in the basin increasing the salinity (and density) of the outflowing AdDW into the IS that gradually impairs the cyclonic NIG, eventually reversing it to an anticyclone.

The physical and biogeochemical data presented here were measured by surface sensors deployed at the EMSO-E2M3A regional facility. The site is located in the center of the SAP (nominal position 41.5053°N, 18.0806°E; Figure 1a) and it is composed of two independent mooring lines (Figure 1b). The primary mooring line hosts a surface buoy allowing real-time transmission of meteorological, and ocean surface hydrological and biogeochemical data. The secondary mooring is composed of an array of sensors positioned at several depths aimed at measuring physical and biogeochemical parameters, from the seafloor to the upper layer (Cardin et al., 2025a). Further information on the site can be found in Bozzano et al. (2013) and Ravaioli et al. (2016).

ha formattato: Colore carattere: Rosso

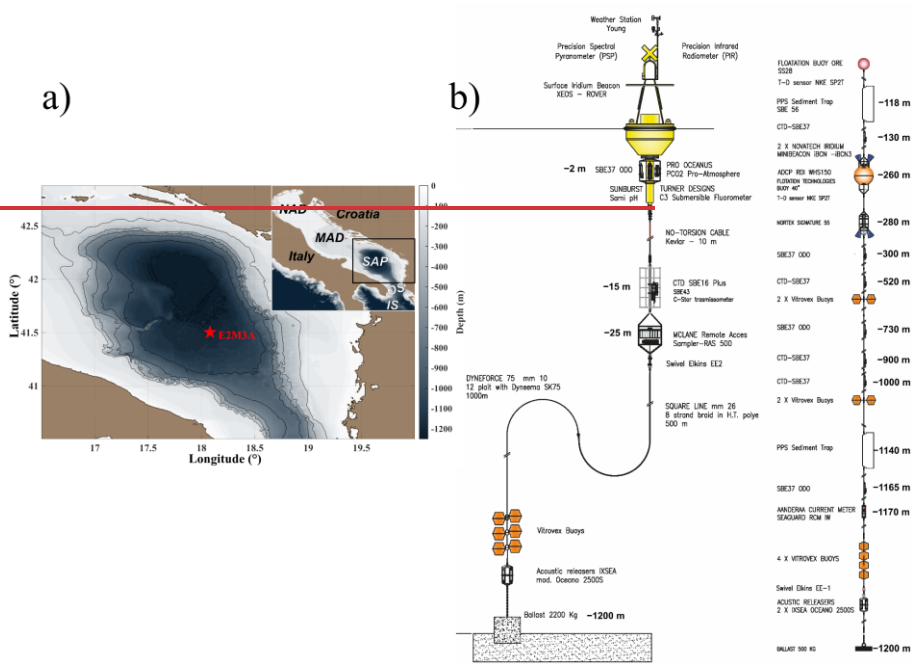



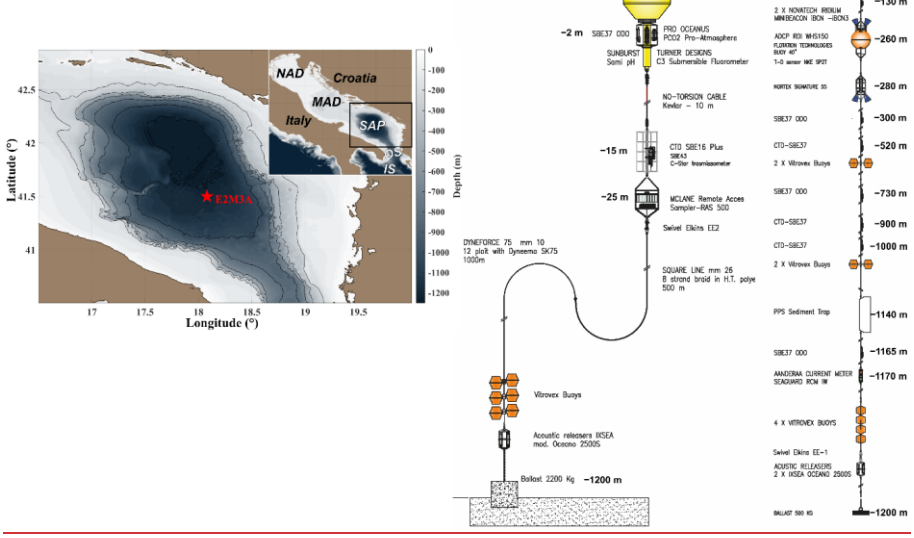
a)
b)
NAD
Croatia
MAD
Italy
SAP
IS
E2M3A
Latitude (°)
Longitude (°)
Depth (m)
Weather Station Young
Precision Spectral Pyranometer (PSP)
Precision Infrared Radiometer (PIR)
Surface Iridium Beacon XEOS – ROVER
-2 m SBE37 ODO
PRO OCEANUS PCO2 Pro-Atmosphere
SUNBURST Semi pH
TURNER DESIGNS C3 Submersible Fluorometer
NO-TORSION CABLE Kevlar – 10 m
-15 m
CTD SBE16 Plus SBE43 C-Star transmissometer
-25 m
MCLANE Remote Acces Sampler-RAS 500
Swivel Elkins EE2
DYNEFORCE 75 mm 10 12 plait with Dyneema SK75 1000m
SQUARE LINE mm 26 8 strand braid in H.T. polye 500 m
Vitrovex Buoys
Acoustic releasers IXSEA mod. Oceano 2500S
Ballast 2200 Kg -1200 m
FLOATATION BUOY ORE SS2B
T-D sensor NKE SP2T
PPS Sediment Trap SBE 56
CTD-SBE37
2 X NOVATECH IRIDIUM MINIBEACON IBCN -IBCN3
ADCP RDI WHS150
FLOATATION TECHNOLOGIES BUOY 40"
NORTEK SIGNATURE 55
SBE37 ODO
2 X Vitrovex Buoys
PPS Sediment Trap
AANDERAA CURRENT METER SEAGUARD RCM 9M
4 X VITROVEX BUOYS
Swivel Elkins EE-1
ACUSTIC RELEASERS 2 X IXSEA OCEANO 2500S
BALLAST 500 KG
-118 m
-130 m
-260 m
-280 m
-300 m
-520 m
-730 m
-900 m
-1000 m
-1140 m
-1165 m
-1170 m
-1200 m

**Figure 1.** a) Map of the study area with the location of EMSO-E2M3A station (nominal position 41.5053°N, 18.0806°E) represented by the red star moored in the South Adriatic Pit. Geographical indications of the Southern Adriatic Pit (SAP), the Otranto Strait (OS), Ionian Sea (IS), Middle Adriatic (MAD) and northern Adriatic (NAD) are provided. b) Scheme of the surface buoy and of the deep mooring with the depths of the different instruments.

ha formattato: Colore carattere: Rosso

### 2.2. Data collection and quality check

Time series from autonomous sensors at key locations are fundamental components of the GOOS (https://www.ioc.unesco.org/). They provide a continuous view of the temporal behaviour of the system on long-term baselines, enabling the measurement of a wide range of interrelated variables, promoting the sharing of data, as demonstrated by international initiatives such as MonGOOS (The Mediterranean Oceanographic Network for the Global Ocean Observing System), OceanSITES and FixO3 (Fixed point Open Ocean Observatory network, FP7 EUProject). Nevertheless, the data, acquired by sensors on ocean observing infrastructures, require quality controls according to defined standards to serve as reliable reference points. In the next sections, a detailed description of the data quality procedures applied to the data will be discussed.

ha formattato: Colore carattere: Rosso

ha formattato: Colore carattere: Rosso

#### 2.2.1. Meteorological data

Meteorological high-frequency (hourly) data were collected by Young (R.M. Young Company) sensors on the meteorological station located on the surface buoy. These data include: air temperature (°C), wind speed (m/s), wind gust (m/s), wind direction (°deg), air pressure (hPa), relative humidity (%) and long and short wave radiation ($W/m^2$). Horizontal wind speed and direction have been measured by a Wind Monitor-MA (model 05106), with manufacturer stated accuracy of ± 0.3 m/s and ± 3 degrees respectively, pressure is measured by a barometric pressure sensor (model 61402V) with manufacturer stated digital accuracy of 0.2 hPa (at 25°C) and 0.3 hPa (-40°C to +60°C) and analog accuracy of 0.05% of analog pressure range, and relative humidity and air temperature were measured by a Relative Humidity/Temperature Probe (model 41382VC) with manufacturer stated accuracy equals to ± 0.1% (at 23°C) and ± 0.3°C (at 23°C) respectively. Data have been corrected and quality controlled following the procedure described in Cardin et al. (2014). This procedure consists of a series of tests on the data to identify erroneous and anomalous values to establish if the data have been corrupted. Checks on individual or consecutive data points provide information for instrument errors, and checks on regional ranges, consistency with physical limits of the data (spikes), rate of change, and stationarity of data were also performed. No editing of invalid data and replacement of missing data are performed, but only a flag is given to the data at each of the automatic quality control checks.

ha formattato: Colore carattere: Rosso

ha formattato: Colore carattere: Rosso

ha formattato: Colore carattere: Rosso

#### 2.2.2. CTD data

Temperature (°C), salinity (Sal) and dissolved oxygen (DO, µmol/kg) high-frequency data (hourly) were collected by a CTD (Conductivity-Temperature-Depth) SeaBird SBE 37-ODO probe at 2 m depth. The SBE 37-ODO is a high-accuracy conductivity and temperature recorder that includes an Optical Dissolved Oxygen (DO) sensor (SBE63). The instrument has ~~a manufacturer~~a manufacturer stated accuracy of ± 0.002 °C, ± 0.003 mS/cm and ± 0.1% of full scale, for temperature, conductivity and oxygen respectively. The data underwent an initial quality control as described in Cardin et al. (2014). First, a physical range test is applied to the data to control the physical

significance of each parameter. Given the general increase in salinity in the SAP, as reported by Amorim et al. (2024) and Le Meur et al. (2025), a modified salinity threshold than Cardin et al., (2014) was applied (39.5 instead of 39). Despiking was then performed to highlight the values having a difference with neighbouring values greater than the defined threshold. Finally, a rate of change test was performed as the final step of the initial quality control procedure. While despiking identifies isolated outliers that differ significantly from the neighbouring values, the rate of change identifies fluctuations that are too rapid. After this step, linear interpolation was applied to data gaps greater than 6 hours. While the first quality control consisted of statistical analyses, the second quality control procedure focused on the comparison between SBE 37-ODO time series and reference data collected during oceanographic cruises. For temperature and conductivity (salinity), fourteen corrected CTD casts performed near EMSO-E2M3A from 02/11/2015 to 31/10/2024 were used. The CTD casts were corrected according to the post-processing methods suggested by the manufacturer (SeaBird software). These CTD casts were taken as reference as they have a higher accuracy and higher vertical resolution than the data measured by the SBE 37-ODO. The time series were compared with the reference CTD casts to detect any offset, which, if present, was added to the time series. Another type of error that can affect a time series and needs to be corrected is the drift of the instrument. Particular attention should be paid to the natural variability and trend of the different variables characterizing the dynamics occurring in the area. In this case, the drift was calculated considering both short time periods, and the entire time span of the SBE 37-ODO time series. Calculating the drift only over a short time scale, that may result from an episodic physical process, is not representative of the long-term natural trend. DO (µmol/kg) data were quality checked by comparing the probe data with DO (µmol/kg) from discrete samples collected at the EMSO-E2M3A station. Samples for the determination of DO were collected in calibrated 50 ml bottles and DO was determined by the Winkler potentiometric titration method (Oudot et al., 1988). The precision of the measurements was evaluated on three to five replicates collected from the same Niskin bottle, and was, on average, 0.08%. Before the comparison with reference seawater samples, post-processing of DO data follows the same quality control procedures applied to temperature and conductivity (salinity). However, an additional quality control step for DO was introduced before the second quality control to account for the adjustment time of the oxygen sensor at switch-on. It consisted of fitting a double exponential function and flagging initial values that deviated significantly from the long-term behavior. The comparison was possible with a limited number of samples, which revealed a mean difference between DO from discrete samples and DO measured by the probe of -9.36 µmol/kg (-0.21 mL/L) with a maximum difference of -10.35 µmol/kg (-0.232 mL/L). Further information on the correction methods applied can be found in Bensi et al., (2012, 2014), Cardin et al. (2020), Amorim et al., (2024) and Le Meur et al., (2025).

**ha formattato:** Colore carattere: Rosso

**ha formattato:** Colore carattere: Rosso

**ha formattato:** Colore carattere: Rosso

**ha formattato:** Colore carattere: Rosso

#### 2.2.3. Sea surface $pCO_2$

Since 2014, a Pro-Oceanus $CO_2$-Pro sensor has provided high-frequency (every 4 hours) autonomous measurements of $pCO_2$ in water ($pCO_{2sw}$, µatm) at a depth of approximately 2 meters. In 2023, a Pro-Oceanus $CO_2$-Pro ATM sensor was deployed, allowing high-frequency (every 4 hours) continuous measurements of $pCO_{2sw}$ and atmospheric $pCO_2$ ($pCO_{2atm}$, µatm) in alternating mode. Pro-Oceanus $CO_2$ sensors measure dissolved $CO_2$ with a semi-permeable membrane, allowing $CO_2$ in the gas phase to equilibrate with the surrounding water. The 'wet' $CO_2$ concentration ($xCO_2$, ppmv) is then detected by an infrared sensor, and the $pCO_{2sw}$ (in µatm) is

**ha formattato:** Colore carattere: Rosso

**ha formattato:** Colore carattere: Rosso

calculated by multiplying this concentration by the total pressure, in millibars (mbar), within the instrument's gas stream:

$$pCO_{2sw} = xCO_2 \; x \; \frac{P}{1013.25} \quad (1)$$

Long-term signal stability of the data is achieved by an automatic zero compensation function that removes $CO_2$ from the system at regular intervals and records a new $CO_2$ baseline value. Both sensors ($CO_2$-Pro and $CO_2$-Pro ATM) have a manufacturer stated accuracy of ± 5 µatm. As the first step in the data quality control procedure, the auto-calibration values following the automatic zero adjustment were discarded. If no stability of the measurements was detected, also the second and, in some cases, the third values after the automatic zero were removed. In addition, outliers resulting from sensor malfunctions or maintenance operations were removed. Calibration by vendors and pre and post deployment checks of the sensors were regularly performed at the in-house laboratory at OGS, the Calibration and Metrology Center (CTMO), to ensure the quality of the measurements presented here. Additionally, reference water samples of pH and total alkalinity were collected near the sensor for the calculation of $pCO_{2sw}$. These samples were collected during the annual visits to the EMSO-E2M3A observatory. Calculations were performed using the CO2SYS software (Pierrot et al., 2006) with the carbonic acid equilibrium constants (K1 and K2) from Lueker et al. (2000), the dissociation constant for $HSO_4$ from Dickson et al. (1990) and the borate dissociation constant from Lee et al. (2010). The $pCO_{2sw}$ from discrete samples ($pCO_{2sw@sample}$, µatm) was matched with the closest hourly $pCO_{2sw}$ from sensor ($pCO_{2sw@probe}$, µatm) resulting in the comparison of seven data points in the period 2015 - 2024 (Table 1). When matching within this short time interval was not possible, a comparison between the $pCO_{2sw@sample}$ and the $pCO_{2sw@probe}$ with a difference of a few days (no more than one week) was performed. To ensure comparability, $pCO_{2sw@probe}$ was adjusted to the temperature measured at the time of seawater sampling, which was also used for the determination of $pCO_{2sw@probe}$, according to Takahashi et al., (1993):

$$pCO_{2sw@Tadj} = pCO_{2sw@probe} \; x \; exp^{(0.0423 \; x \; (T_{probe} - T_{sample}))} \quad (2)$$

where $pCO_{2sw@Tadj}$ (µatm) is the $pCO_{2sw}$ probe value adjusted for the temperature difference, $pCO_{2sw@probe}$ is the $pCO_{2sw}$ measured by the probe (µatm), $T_{probe}$ is the temperature (°C) measured by the SeaBird SBE 37-ODO during the acquisition of the $pCO_{2sw@probe}$ and $T_{sample}$ is the temperature (°C) measured by the CTD casts during the collection of the discrete samples.

**Table 1**. Comparison between $pCO_{2sw}$ from discrete samples ($pCO_{2sw@sample}$, µatm) and $pCO_{2sw}$ from probe ($pCO_{2sw@probe}$, µatm). The difference is calculated as $pCO_{2sw@sample}$ - $pCO_{2sw@probe}$.

| Date | $pCO_{2sw@samples}$ (µatm) | $pCO_{2sw@probe}$ (µatm) | Difference (µatm) |
|---|---|---|---|
| 20/10/2014 | 328.11 | 361.23 | -33.12 |

ha formattato: Colore carattere: Rosso

ha formattato: Colore carattere: Rosso

| | | | |
|---|---|---|---|
| 29/10/2015 | 381.46 | 382.63 | -1.17 |
| 29/07/2017 | 486.74 | 480.40 | 6.34 |
| 08/10/2018 | 381.26 | 397.50 | -16.34 |
| 19/10/2019 | 399.33 | 379.15 | 20.18 |
| 30/10/2022 | 383.45 | 420.90 | -37.45 |
| 05/12/2023 | 361.00 | 364.64 | -3.64 |

In three out of seven cases, the accuracy of the measurements falls within either the manufacturer's stated accuracy (±5 µatm) or the target accuracy defined by the ICOS network for Fixed Ocean Stations (±10 µatm, https://www.icos-otc.org/). In all other cases, these criteria were not met. However, during the recent ICOS Ocean Thematic Centre (OTC) $pCO_2$ inter-comparison experiment (Steinhoff et al., 2025), it was demonstrated that deviations of around 15 - 20 µatm can be expected by membrane sensors, particularly under conditions of increasing temperature. Additionally, in the two cases of very high deviation, biofouling-likely developing during the spring/summer period could be identified as a probable contributing factor for this difference. Indeed continuous monitoring and maintenance of open ocean fixed observatories is often constrained by available infrastructure, and strict ship time windows influenced by several factors such as weather conditions (Coppola et al., 2016). Additionally, in 2020, $pCO_{2sw}$ measurements were acquired by two Unmanned Surface Vehicles (USVs) from Saildrone Inc. (USA) during the ATL2MED demonstration experiment around the EMSO-E2M3A observatory (Martellucci et al., 2024a; 2025). One of the saildrone was equipped with an ASVCO2 system developed by PMEL (NOAA's Pacific Marine Environmental Laboratory). This system fed seawater in a bubble equilibrator (Friederich et al., 1995), and the partially dried $xCO_2$ is measured with an infrared detector (LI-COR 820 $CO_2$ gas analyser). A two-point calibration was used, where the first is a reference gas from NOAA/ESRL, while the second is air purged for $CO_2$. Detailed description of the correction, adjustment and quality of $pCO_{2sw}$ Saildrone data can be found in Martellucci et al. (2024a). A similar trend (significant correlation coefficient of 0.77, p-value < 0.01) and a constant offset of 16 µatm between the Saildrone and EMSO-E2M3A data were reported, providing an additional line of evidence for the reliability of this dataset.

Due to the limited number of reference water samples and their incomplete representation of the full $CO_2$ annual cycle, no corrections to the $pCO_{2sw}$ data were applied.

#### 2.2.4. pH data

Hourly pH data were obtained from a SAMI-pH sensor deployed at a depth of 2 meters, covering a two-year period from 2015 to 2016. The instrument uses a high-accuracy colorimetric method, in which seawater is pumped through the sensor and mixed with a pH-sensitive indicator solution (meta-Cresol Purple). According to certified reference material (CRM) intercomparisons, the sensor provides an accuracy of ± 0.003 pH units and a precision of about 0.001 pH units. Calibration by vendors and pre deployment checks of the sensor were performed by the OGS CTMO facility. Discrete samples in the region were also collected in 2015, but no cruises were conducted in the region in 2016. Water samples for validation were collected in 250 mL borosilicate bottles and preserved with mercury chloride ($HgCl_2$) to prevent biological activity. Samples were stored in the dark and kept cool until

laboratory analysis at the OGS facilities. Total scale pH ($pH_T$) was determined spectrophotometrically following the standard operating procedure SOP 6b described in Dickson et al. (2007). Analyses were performed using a Cary 100 Scan UV-Visible spectrophotometer with a 10 cm pathlength cylindrical quartz cell and a purified 4 mM m-Cresol Purple indicator dye. Prior to measurement, samples were equilibrated to 25°C, then subsampled by siphoning through a Tygon tube to avoid gas exchange, ensuring no headspace was present in the cuvette. $pH_T$ was measured immediately after sub-sampling. The precision of the measurements was evaluated on three to five replicates collected from the same Niskin bottle, and was, on average, 0.01%. During the analysis, the temperature of the samples was controlled using a thermostatic cell holders inside the spectrophotometer, connected to a circulation criothermostat (LAUDA RE415) and monitored with a digital thermometer (VWR Traceable). The mean difference between the three discrete samples and the probe measurements was equal to -0.05 pH units. No further correction to the time series was applied.

## 3. Robustness and seasonal consistency of the dataset

The surface dataset presented here has been carefully corrected (physical data) and validated (meteorological, $pCO_2$ and pH data), as described in the previous sections, and all data are publicly available (https://doi.org/10.13120/y2hw-1j63, Cardin et al., 2025b). Data gaps were due to maintenance operations, malfunctioning of the sensors and/or the removal of measurements that failed the quality-control procedures described in previous sections. The resulting $pCO_{2sw}$ time series (Figure 2a) falls within the expected range of variability for the region. Both the values and seasonal amplitudes are consistent with previous observations in different regions of the Mediterranean Sea (e.g., Pecci et al., 2024; Garcia-Ibañez et al., 2024; Frangoulis et al., 2024: Coppola et al., 2020; Merlivat et al., 2018) and in the Adriatic Sea (e.g., Turk et al., 2010; Cantoni et al., 2012; Ingrosso et al., 2016; Urbini et al., 2020; Cantoni et al., 2024). Lower values are observed in winter, with $pCO_{2sw}$ concentrations ranging between 350 and 400 µatm, mainly due to the cooling of the sea surface layer. However, during periods of winter convection and enhanced vertical mixing, $pCO_{2sw}$ increases, as observed between December and February in the 2017–2018, 2020–2021, and 2023–2024 periods. In contrast, summer values were around 500 µatm, and in 2022 rise above 550 µatm, closely following surface warming and stratification. Alongside $pCO_{2sw}$, other physical and biogeochemical parameters measured at the site further describe the surface layer dynamics. Temperature reflects the seasonal alternation between winter mixing and summer stratification, with values ranging, on average, from 14.87 °C in winter to 25.39 °C in summer (Figure 2b). Particularly high temperatures were recorded in 2015, when summer maxima reached 29.6 °C in July. In the following years, summer temperatures remained close to the seasonal average. Interestingly, winter minima showed a gradual increase over time, from values near the seasonal average in the period 2016 - 2019 to an average of around 15.04 °C starting from 2021. Overall, surface temperatures appear slightly higher than those reported for the northwestern Mediterranean (Garcia-Ibañez et al., 2024), especially during the summer months. Marked interannual variability characterizes salinity (Figure 2c), with maximum values exceeding 39 in several years (for instance in 2017, 2020, 2021 and 2022) consistent with previously reported values in the SAP (e.g., Mihanović et al., 2021; Menna et al., 2022). These salinity values are typically higher than those observed in the central Mediterranean (e.g., Lampedusa site, Pecci et al., 2024) or the northwestern Mediterranean (Garcia-Ibañez et al., 2024) reflecting the influence of warm, saline waters of Levantine/Cretan origin entering the area (see Sect. 2.1). Oxygen concentrations follow the expected seasonal dynamics (Figure 2d): lower values are shown during winter

**ha formattato:** Colore carattere: Rosso

**ha formattato:** Colore carattere: Rosso

**ha formattato:** Colore carattere: Rosso

**ha formattato:** Colore carattere: Rosso

**ha formattato:** Colore carattere: Rosso

**ha formattato:** Colore carattere: Rosso

**ha formattato:** Colore carattere: Rosso

mixing, when ventilation dominates, followed by an increase (first peak in the time series) that corresponds to the post-convection bloom. In summer, oxygen concentration decreases again due to respiration processes (e.g., Martellucci et al., 2024b). Finally, DO increases again at the end of summer (second peak in the time series) due to a smaller bloom occurring in the region during late summer/autumn. Wind speed data (Figure 2e) are also consistent with the regional mean values (e.g., Turk et al., 2010; Pecci et al., 2024) and underline the role of atmospheric forcing in sustaining vertical exchanges, particularly in winter. Mean wind speed value was 5.12 m/s but being frequently higher than 10 m/s. Nevertheless, here an assessment of the main wind regimes in the southern Adriatic was not performed as it was beyond the scope of this manuscript.

**ha formattato:** Colore carattere: Rosso

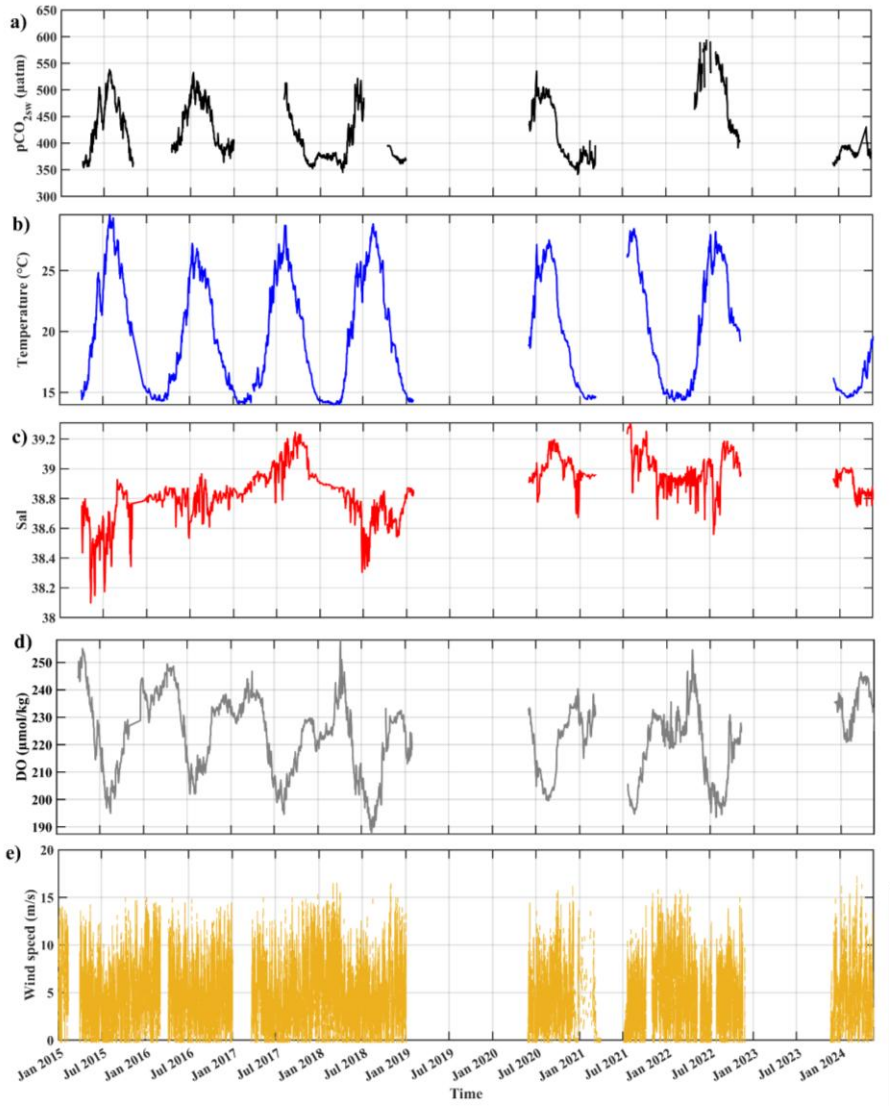


**Figure 2.** Time series of sea surface a) partial pressure of CO2 ($pCO_{2sw}$ in µatm); b) Temperature (°C); c) Salinity (Sal); d) dissolved oxygen (DO in µmol/kg); and e) Wind speed (m/s). The variables were measured in the period 2015 - 2024 at EMSO-E2M3A observatory. Periods of missing data were due to maintenance operations, malfunctioning of the sensors and/or the removal of measurements that failed the quality-control procedures described in Sect. 2.2..

A summary of the main biogeochemical and hydrographic variability reported in other Mediterranean regions from fixed ocean stations in recent years is provided in Table 2.

**ha formattato:** Colore carattere: Rosso

**Table 2**. Summary of $pCO_{2sw}$ and hydrographic variability in other oceanographic regions of the Mediterranean sea.

| Observational site | Time span | $pCO_{2sw}$ | Hydrography | Dissolved oxygen | Wind speed | References |
|---|---|---|---|---|---|---|
| Lampedusa Oceanographic Observatory (Central Mediterranean sea) | December 2021 - June 2023 | Seasonal variability: 350 µatm (winter) and 525 µatm (summer) | Salinity ranges: 36.9 - 38.2<br><br>Sea surface temperature ranges: 16°C (winter) and 29°C (summer) | - | Wind speed ranges: between 0 m/s and 15 m/s | Pecci et al., 2024 |
| L'Estartit Oceanographic Station and the Blanes Bay Microbial Observatory (Northwestern Mediterranean Sea) | January 2010 - August 2019 | Seasonal variability ($fCO_2$): 350 µatm (winter) and 500 µatm (summer) | Salinity ranges: no clear seasonal cycle, values around 37.9 ± 0.3<br><br>Sea surface temperature ranges: 13°C (winter) and 23°C (summer) | - | - | Garcia-Ibañez et al., 2024 |
| BOUSSOLE and DYFAMED sites (Ligurian Sea) | 1995–1997 and February 2013 - February 2015 | Seasonal variability ($fCO_2$): 350 µatm (winter) and > 550 µatm (summer) in the 2013 - 2015 period | Mean salinity: values around 38.21 ± 0.03 (1995 - 1997) and 38.19 ± 0.02 (2013 - 2015)<br><br>Sea surface temperature ranges: 13°C (winter) and 27°C (summer) | - | - | Coppola et al., 2020; Merlivat et al., 2018 |
| POSEIDON fixed platform (Eastern Mediterranean Sea) | January 2020 - May 2023 | Seasonal variability: 350 µatm (winter) and ~500 µatm (summer) | Salinity ranges: 39 - 39.6<br><br>Sea surface temperature ranges: 15.3°C (winter) and 28.3°C (summer) | - | - | Frangoulis et al., 2024 |
| Gulf of Trieste (Northern Adriatic Sea) | 2007-2008; 2008 - 2009; 2011-2013; 2014-2017 | Seasonal variability: 220 µatm (winter) and between 475 µatm and 500 µatm (summer) | Salinity ranges: 36 - 37.5 but strong influence of rivers (values < 36)<br><br>Sea surface temperature ranges: 8°C (winter) and between 26 and 29.5°C (summer) | Dissolved oxygen range: 270 µmol/kg (winter) and around 200 µmol/kg (summer) | Wind speed ranges: between 0 m/s and 15 m/s | Turk et al., 2010; Cantoni et al., 2012; Ingrosso et al., 2016; Urbini et al., 2020; Cantoni et al., 2024 |

**ha formattato:** Colore carattere: Rosso

Overall, the consistency of seasonal and interannual patterns, and their alignment with well-known physical and biogeochemical drivers such as convection, stratification, and biological activity, strongly support the reliability

of the dataset. These results reinforce the robustness of the observations and provide a solid basis for further scientific interpretation.

## 4. Extended and potential future applications of the dataset: calculation of atmospheric carbon flux ($FCO_2$)

The dataset presented here can be used to describe physical and biogeochemical properties of surface water in the SAP, as well as to estimate the atmospheric carbon flux ($FCO_2$). This is essential for evaluating the role of the SAP as a potential carbon source or sink across various temporal scales. Ensuring the reliability of air–sea $CO_2$ flux calculations requires careful evaluation of atmospheric $pCO_2$ and wind speed data, as different parameterizations may need to be applied and some input data recalculated to meet the requirements of the $FCO_2$ formulation. In particular, different parameterizations of the gas transfer velocity could yield divergent results. Equally important is the quality of $pCO_{2sw}$ data from sensors. As reported in Steinhoff et al. (2025), it is essential to have a certain degree of knowledge and expertise to produce and interpret optimal quality data, especially for membrane-based systems (such as the submersible Pro-Oceanus sensors) that are easier to operate in the field but require critical understanding of the instrument's characteristics for data processing. Careful validation and quality control of these input parameters are therefore essential. Addressing these methodological considerations is a prerequisite for producing credible flux estimates and, ultimately, for advancing the understanding of carbon dynamics in the SAP.

## 5. Data availability

Data described in this work are freely available at the National Oceanographic Data Center (NODC) of the National Institute of Oceanography and Applied Geophysics (https://doi.org/10.13120/y2hw-1j63, Cardin et al., 2025b).

## 6. Conclusions

High frequency observations from fixed stations, such as surface buoys and/or moorings, play a crucial role in assessing the regional variability of the carbon cycle in the Mediterranean Sea across different time scales. The dataset presented here provides a comprehensive resource for exploring the biogeochemical and physical dynamics of the sea surface in the dense water formation area of the southern Adriatic Sea. For the first time, high-frequency observations of meteorological, hydrographic and seawater $pCO_2$ and pH data are presented. In addition, the methods used to perform quality control (QC) of the data and possible improvements are discussed. QC is particularly important for $pCO_{2sw}$ data as many challenges (such as strict ship time windows) were faced in the region as discussed in Sect. 2.2. Making this time series available for the first time is a significant advancement, particularly considering the strategic importance of the region as a key dense water formation area and for air-sea interaction which are fundamental mechanisms for the capture and storage of atmospheric $CO_2$. Thus, this dataset provides a valuable example for estimating local surface hydrological and biogeochemical dynamics based on high-resolution regional observations with a high degree of accuracy. This dataset could be also used to characterize carbon flux at the surface in the SAP using only in situ observations, explicitly estimating uncertainties associated with the input variables for $CO_2$ flux calculations (Sect. 4). In particular, uncertainty related to key parameters such as atmospheric $pCO_2$ and wind speed, which are typically derived from other

ha formattato: Colore carattere: Rosso
ha formattato: Colore carattere: Rosso
ha formattato: Colore carattere: Rosso
ha formattato: Colore carattere: Rosso
ha formattato: Colore carattere: Rosso
ha formattato: Colore carattere: Rosso

observatories or retrieved from models (Ulses et al., 2023). However, some of the data ($pCO_{2atm}$) currently cover only limited time periods, making data integration necessary to ensure consistency in flux estimates.

**Author contribution.**

CD: data curation, investigation, validation, writing (original draft), writing (review and editing), conceptualisation, formal analysis, software. AR: investigation, writing (review and editing), conceptualisation. GCi: data curation, investigation, validation, writing (review and editing), conceptualisation. MG: data curation, investigation, validation, writing (review and editing), conceptualisation. GCo: investigation, writing (review and editing), conceptualisation. GS: data curation, writing (review and editing), validation, software. SK: data curation, writing (review and editing), validation, software. JLM: data curation, validation, writing (review and editing), software. VC: funding acquisition, project administration, data curation, investigation, validation, writing (review and editing), conceptualisation, supervision.

**Competing interests.** The contact author has declared that none of the authors has any competing interests.

**Acknowledgement.**

This work benefited from access to E2M3A South Adriatic Regional facility, an EMSO-IT/ICOS-IT and EMSO-ERIC and ICOS Site, operated by OGS. Dataset and activities were partially funded by EMSO Italian Joint Research Unit, by OGS and by the EU - Next Generation EU Mission 4, Component 2, Investment 3.1, "Fund for the realisation of an integrated system of research and innovation infrastructures," for Project IR0000032 – ITINERIS - Italian Integrated Environmental Research Infrastructures System. The authors express their gratitude to the PHYS, BIO and TEC teams, as well as the CTMO units of OGS and to the CNR-ISP, for their essential contributions and continuous efforts in operating and maintaining the EMSO/ICOS-E2M3A regional facility. The authors thank Christian Puntini for his valuable contribution to curating the meteorological data. The author also acknowledges the creators of ChatGPT, used to improve the English writing in some parts of this manuscript.

**References**

Alvarez, M., Catala, S.T., Civitarese, G., Coppola, L., Hassoun, A., Ibello, V., Lazzari, P., Lefevre, D., Macias, D., Santinelli, C., and Ulse, C.: Mediterranean Sea general biogeochemistry, In: Oceanography of the Mediterranean Sea, edited by: Schroeder, K., and Chiggiato, J0., Elsevier, Amsterdam, pp. 387 –451, https://doi.org/10.1016/B978-0-12-823692-5.00004-2, 2023.

Amorim, F. L. L., Le Meur, J., Wirth, A., and Cardin, V.: Tipping of the double-diffusive regime in the southern Adriatic Pit in 2017 in connection with record high-salinity values, Ocean Sci., 20, 463–474, https://doi.org/10.5194/os-20-463-2024, 2024.

Artegiani, A., Paschini, E., Russo, A., Bregant, D., Raicich, F., and Pinardi, N.: The Adriatic Sea General Circulation. Part I: Air–Sea Interactions and Water Mass Structure, J. Phys. Oceanogr., 27, 1492–1514, https://doi.org/10.1175/1520-0485(1997)027<1492:tasgcp>2.0.co;2, 1997.

Bensi, M.: Thermohaline variability and mesoscale dynamics observed at the E2M3A deep-site in the south Adriatic sea, PhD thesis, Università degli studi di Trieste, Italy, 2012.

ha formattato: Colore carattere: Rosso

ha formattato: Colore carattere: Rosso

Bensi, M., Cardin, V., Rubino, A., Notarstefano, G., and Poulain, P. M.: Effects of winter convection on the deep layer of the Southern Adriatic Sea in 2012: Effects of strong shelf convection, J. Geophys. Res. Oceans, 118, 6064–6075, https://doi.org/10.1002/2013jc009432, 2013.

Bensi, M., Cardin, V., and Rubino, A.: Thermohaline variability and mesoscale dynamics observed at the deep-ocean observatory E2M3A in the southern Adriatic sea, in The Mediterranean Sea: Temporal Variability and Spatial Patterns, Geophysical Monograph Series, eds G. L. E. Borzelli, M. Gačić, P. Lionello, and P. Malanotte-Rizzoli (Oxford, UK: John Wiley & Sons, Inc.), 139–155, https://doi.org/10.1002/9781118847572.ch9, 2014.

Bignami, F., Salusti, E., and Schiarini, S.: Observations on a bottom vein of dense water in the southern Adriatic and Ionian seas, J. Geophys. Res., 95, 7249–7259, https://doi.org/10.1029/jc095ic05p07249, 1990.

Bozzano, R., Pensieri, S., Pensieri, L., Cardin, V., Brunetti, F., Bensi, M., Petihakis, G., Tsagaraki, T. M., Ntoumas, M., Podaras, D., and Perivoliotis, L.: The M3A network of open ocean observatories in the Mediterranean Sea, in: 2013 MTS/IEEE OCEANS-Bergen, IEEE, Bergen, Norway, 10–14 June 2013, 1–10, https://doi.org/10.1109/OCEANS-Bergen.2013.6607996, 2013.

Bunsen, F., Nissen, C., and Hauck, J.: The Impact of Recent Climate Change on the Global Ocean Carbon Sink, Geophysical Research Letters, 51, https://doi.org/10.1029/2023gl107030, 2024.

Cantoni, C., Luchetta, A., Celio, M., Cozzi, S., Raicich, F., and Catalano, G.: Carbonate system variability in the Gulf of Trieste (North Adriatic Sea), Estuarine, Coastal and Shelf Science, 115, 51–62, https://doi.org/10.1016/j.ecss.2012.07.006, 2012.

Cantoni, C., Luchetta, A., Chiggiato, J., Cozzi, S., Schroeder, K., and Langone, L.: Dense water flow and carbonate system in the southern Adriatic: A focus on the 2012 event, Marine Geology, 375, 15–27, https://doi.org/10.1016/j.margeo.2015.08.013, 2016.

Cantoni, C., De Vittor, C., Faganeli, J., Giani, M., Kovač, N., Malej, A., Ogrinc, N., Tamše, S., and Turk, V.: Carbonate system and acidification of the Adriatic Sea, Marine Chemistry, 267, 104462, https://doi.org/10.1016/j.marchem.2024.104462, 2024.

Cardin, V., Bensi, M., and Pacciaroni, M.: Variability of water mass properties in the last two decades in the South Adriatic Sea with emphasis on the period 2006–2009, Continental Shelf Research, 31, 951–965, https://doi.org/10.1016/j.csr.2011.03.002, 2011.

Cardin V., Siena, G., Giorgetti, A., Ursella, L., Brosich, A., and Partescano, E.: The Ritmare Fixed Sites Network Procedures for Real-Time Data Quality Control, https://doi.org/10.13140/RG.2.2.31100.44166, 2014.

Cardin, V., Wirth, A., Khosravi, M., and Gačić, M.: South Adriatic Recipes: Estimating the Vertical Mixing in the Deep Pit, Front. Mar. Sci., 7, https://doi.org/10.3389/fmars.2020.565982, 2020.

Cardin, V., Le Meur, J., Ursella, L., Dentico, C., Siena, G., Mansutti, P., Brunetti, F., and Partescano, E.: EMSO-E2M3A-Water-Column-time-series-South-Adriatic [dataset], https://doi.org/10.13120/ZE9Q-3E51, 2025a.

**ha formattato:** Colore carattere: Rosso

**ha formattato:** Colore carattere: Rosso

**ha formattato:** Colore carattere: Rosso

**ha formattato:** Colore carattere: Rosso

Cardin, V., Dentico, C., Brunetti, F., Bubbi, A., Chiaruttini, L., Civitarese, G., Comici, C., Corbo, A., Gerin, R., Giani, M., Kuchler, S., Le Meur, J., Mansutti, P., Savonitto, G. and Siena, G.: EMSO-E2M3A-B-Surface-time-series-South-Adriatic [dataset], https://doi.org/10.13120/y2hw-1j63, 2025b.

Civitarese, G., Gačić, M., Batistić, M., Bensi, M., Cardin, V., Dulčić, J., Garić, R., and Menna, M.: The BiOS mechanism: History, theory, implications, Progress in Oceanography, 216, 103056, https://doi.org/10.1016/j.pocean.2023.103056, 2023.

Coppola, L., Ntoumas, M., Bozzano, R., Bensi, M., Hartman, S. E., Charcos Llorens, M., Craig, J., Rolin, J-F., Giovanetti, G., Cano, D., Karstensen, J., Cianca, A., Toma, D., Stasch, C.,Pensieri, S., Cardin, V., Tengberg, A., Petihakis, G., and Cristini, L.: Handbook of Best Practices for Open Ocean Fixed Observatories, FixO3 Project, 127, FP7 Programme 2007–2013 under grant agreement no 312463, European Commission, 2016.

$CO_2$.Earth: http://co2.earth/, last access: 14 July 2025.

Dickson, A.G.: Therodynamics of the dissociation of boric acid and synthetic seawater from 273.15 to 318.15 K. Deep -Sea Res. 137, 755 –766, 1990.

Dickson, A., Sabine, C., and Christian, J.R.: Guide to best practice for ocean CO 2 measurements. PICES Special Pubbl. 3, 2007.

Fedele, G., Mauri, E., Notarstefano, G., and Poulain, P. M.: Characterization of the Atlantic Water and Levantine Intermediate Water in the Mediterranean Sea using Argo Float Data. Ocean Science Discussions, 1-41, https://doi.org/10.5194/os-18-129-2022, 2021.

Frangoulis, C., Stamataki, N., Pettas, M., Michelinakis, S., King, A. L., Giannoudi, L., Tsiaras, K., Christodoulaki, S., Seppälä, J., Thyssen, M., Borges, A. V., and Krasakopoulou, E.: A carbonate system time series in the Eastern Mediterranean Sea. Two years of high-frequency in-situ observations and remote sensing, Front. Mar. Sci., 11, 1348161, https://doi.org/10.3389/fmars.2024.1348161, 2024.

Friederich, G. E., Brewer, P. G., Herlien, R., and Chavez, F. P.: Measurement of sea surface partial pressure of CO2 from a moored buoy, Deep-Sea Res. Pt. I, 42, 1175–1186, https://doi.org/10.1016/0967-0637(95)00044-7, 1995.

Friedlingstein, P., O'Sullivan, M., Jones, M. W., Andrew, R. M., Hauck, J., Landschützer, P., Le Quéré, C., Li, H., Luijkx, I. T., Olsen, A., Peters, G. P., Peters, W., Pongratz, J., Schwingshackl, C., Sitch, S., Canadell, J. G., Ciais, P., Jackson, R. B., Alin, S. R., Arneth, A., Arora, V., Bates, N. R., Becker, M., Bellouin, N., Berghoff, C. F., Bittig, H. C., Bopp, L., Cadule, P., Campbell, K., Chamberlain, M. A., Chandra, N., Chevallier, F., Chini, L. P., Colligan, T., Decayeux, J., Djeutchouang, L., Dou, X., Duran Rojas, C., Enyo, K., Evans, W., Fay, A., Feely, R. A., Ford, D. J., Foster, A., Gasser, T., Gehlen, M., Gkritzalis, T., Grassi, G., Gregor, L., Gruber, N., Gürses, Ö., Harris, I., Hefner, M., Heinke, J., Hurtt, G. C., Iida, Y., Ilyina, T., Jacobson, A. R., Jain, A., Jarníková, T., Jersild, A., Jiang, F., Jin, Z., Kato, E., Keeling, R. F., Klein Goldewijk, K., Knauer, J., Korsbakken, J. I., Lauvset, S. K., Lefèvre, N., Liu, Z., Liu, J., Ma, L., Maksyutov, S., Marland, G., Mayot, N., McGuire, P., Metzl, N., Monacci, N. M., Morgan, E. J., Nakaoka, S.-I., Neill, C., Niwa, Y., Nützel, T., Olivier, L., Ono, T., Palmer, P. I.,

ha formattato: Colore carattere: Rosso

ha formattato: Colore carattere: Rosso

Pierrot, D., Qin, Z., Resplandy, L., Roobaert, A., Rosan, T. M., Rödenbeck, C., Schwinger, J., Smallman, T. L., Smith, S., Sospedra-Alfonso, R., Steinhoff, T., Sun, Q., et al.: Global Carbon Budget 2024, https://doi.org/10.5194/essd-2024-519, 13 November 2024.

Gačić, M., Marullo, S., Santoleri, R., and Bergamasco, A.: Analysis of the seasonal and interannual variability of the sea surface temperature field in the Adriatic Sea from AVHRR data (1984–1992), J. Geophys. Res., 102, 22937–22946, https://doi.org/10.1029/97jc01720, 1997.

Gačić, M., Civitarese, G., Eusebi Borzelli, G. L., Kovačević, V., Poulain, P.-M., Theocharis, A., Menna, M., Catucci, A., and Zarokanellos, N.: On the relationship between the decadal oscillations of the northern Ionian Sea and the salinity distributions in the eastern Mediterranean, J. Geophys. Res., 116, https://doi.org/10.1029/2011jc007280, 2011.

García-Ibáñez, M. I., Guallart, E. F., Lucas, A., Pascual, J., Gasol, J. M., Marrasé, C., Calvo, E., and Pelejero, C.: Two new coastal time-series of seawater carbonate system variables in the NW Mediterranean Sea: rates and mechanisms controlling pH changes, Front. Mar. Sci., 11, https://doi.org/10.3389/fmars.2024.1348133, 2024.

Gattuso, J-P, and Hansson L. (Eds). Ocean acidification. Oxford university press, 2011.

Hassoun, A. E. R., Gemayel, E., Krasakopoulou, E., Goyet, C., Abboud-Abi Saab, M., Guglielmi, V., Touratier, F., and Falco, C.: Acidification of the Mediterranean Sea from anthropogenic carbon penetration, Deep Sea Research Part I: Oceanographic Research Papers, 102, 1–15, https://doi.org/10.1016/j.dsr.2015.04.005, 2015.

Hassoun, A. E. R., Bantelman, A., Canu, D., Comeau, S., Galdies, C., Gattuso, J.-P., Giani, M., Grelaud, M., Hendriks, I. E., Ibello, V., Idrissi, M., Krasakopoulou, E., Shaltout, N., Solidoro, C., Swarzenski, P. W., and Ziveri, P.: Ocean acidification research in the Mediterranean Sea: Status, trends and next steps, Front. Mar. Sci., 9, https://doi.org/10.3389/fmars.2022.892670, 2022.

ICOS-Ocean Thematic Center: https://www.icos-otc.org/, last access: 14 October 2025.

Intergovernmental Panel on Climate Change (IPCC). Changing State of the Climate System. In: Climate Change 2021 – The Physical Science Basis: Working Group I Contribution to the Sixth Assessment Report of the Intergovernmental Panel on Climate Change. Cambridge University Press; 2023:287-422, 2021.

Ingrosso, G., Giani, M., Comici, C., Kralj, M., Piacentino, S., De Vittor, C., and Del Negro, P.: Drivers of the carbonate system seasonal variations in a Mediterranean gulf, Estuarine, Coastal and Shelf Science, 168, 58–70, https://doi.org/10.1016/j.ecss.2015.11.001, 2016.

Ingrosso, G., Bensi, M., Cardin, V., and Giani, M.: Anthropogenic CO2 in a dense water formation area of the Mediterranean Sea, Deep Sea Research Part I: Oceanographic Research Papers, 123, 118–128, https://doi.org/10.1016/j.dsr.2017.04.004, 2017.

IOC UNESCO: https://www.ioc.unesco.org/en, last access: 21 July 2025.

Kapsenberg, L., Alliouane, S., Gazeau, F., Mousseau, L., and Gattuso, J.-P.: Concomitant ocean acidification and increasing total alkalinity at a coastal site in the NW Mediterranean Sea (2007-2015), https://doi.org/10.5194/os-2016-71, 13 September 2016.

Lazoglou, G., Papadopoulos-Zachos, A., Georgiades, P., Zittis, G., Velikou, K., Manios, E. M., and Anagnostopoulou, C.: Identification of climate change hotspots in the Mediterranean, Sci Rep, 14, 29817, https://doi.org/10.1038/s41598-024-80139-1, 2024.

Lee, K., Kim, T. -W., Byrne, R.H., Millero, F.J., Feely, R.A., Liu, Y -M.: The universal ratio of boron to chlorinity for the North Pacific and North Atlantic oceans. Geochim. Cosmochim. Acta 74, 1801 –1811, 2010.

Lueker, T. J., Dickson, A. G., and Keeling, C. D.: Ocean pCO 2 calculated from dissolved inorganic carbon, alkalinity, and equations for K1 and K2: Validation based on laboratory measurements of CO 2 in gas and seawater at equilibrium. Mar. Chem. 70, 105 –119, 2000.

Le Meur, J., Wirth, A., Paladini De Mendoza, F., Miserocchi, S., and Cardin, V.: Intermittent supply of dense water to the deep South Adriatic Pit: an observational study, Front. Mar. Sci., 12, https://doi.org/10.3389/fmars.2025.1516780, 2025.

Malanotte-Rizzoli, P.: The Northern Adriatic Sea as a prototype of convection and water mass formation on the continental shelf P.C Chu, J.C Gascard (Eds.), Deep Convection and Deep Water Formation in the Oceans, Elsevier Oceanography Series, vol. 57, Elsevier, Amsterdam, pp. 229-239, 1991.

Martellucci, R., Giani, M., Mauri, E., Coppola, L., Paulsen, M., Fourrier, M., Pensieri, S., Cardin, V., Dentico, C., Bozzano, R., Cantoni, C., Lucchetta, A., Izquierdo, A., Bruno, M., and Skjelvan, I.: $CO_2$ and hydrography acquired by autonomous surface vehicles from the Atlantic Ocean to the Mediterranean Sea: data correction and validation, Earth Syst. Sci. Data, 16, 5333–5356, https://doi.org/10.5194/essd-16-5333-2024, 2024a.

Martellucci, R., Menna, M., Mauri, E., Pirro, A., Gerin, R., Paladini De Mendoza, F., Garić, R., Batistić, M., Di Biagio, V., Giordano, P., Langone, L., Miserocchi, S., Gallo, A., Notarstefano, G., Savonitto, G., Bussani, A., Pacciaroni, M., Zuppelli, P., and Poulain, P.-M.: Recent changes of the dissolved oxygen distribution in the deep convection cell of the southern Adriatic Sea, Journal of Marine Systems, 245, 103988, https://doi.org/10.1016/j.jmarsys.2024.103988, 2024b.

Martellucci, R., Dentico, C., Coppola, L., Skjelvan, I., Giani, M., Pensieri, S., Cantoni, C., Cardin, V., Fourrier, M., Bozzano, R., Paulsen, M., and Mauri, E.: Air-sea CO2 exchange in the Eastern Atlantic and the Mediterranean Sea based on autonomous surface measurements, 2025. In review.

Menna, M., Martellucci, R., Notarstefano, G., Mauri, E., Gerin, R., Pacciaroni, M., Bussani, A., Pirro, A., Poulain, P-M.: Record-breaking high salinity in the South Adriatic Pit in 2020, in: Copernicus Ocean State Report, issue 6. Journal of Operational Oceanography, 15(sup1), 1–220. https://doi.org/10.1080/1755876X.2022.2095169, 2022.

**ha formattato:** Colore carattere: Rosso

**ha formattato:** Colore carattere: Rosso

**ha formattato:** Colore carattere: Rosso

Merlivat, L., Boutin, J., Antoine, D., Beaumont, L., Golbol, M., and Vellucci, V.: Increase of dissolved inorganic carbon and decrease in pH in near-surface waters in the Mediterranean Sea during the past two decades, Biogeosciences, 15, 5653–5662, https://doi.org/10.5194/bg-15-5653-2018, 2018.

Mihanović, H., Vilibić, I., Šepić, J., Matić, F., Ljubešić, Z., Mauri, E., Gerin, R., Notarstefano, G., and Poulain, P.-M.: Observation, Preconditioning and Recurrence of Exceptionally High Salinities in the Adriatic Sea, Front. Mar. Sci., 8, 672210, https://doi.org/10.3389/fmars.2021.672210, 2021.

Ovchinnikov, I.M., Zats, V.I., Krivosheya, V.G., and Udodov, A.I.: Formation of deep Eastern Mediterranean waters in the Adriatic Sea. Oceanology, 25, 6, 704-707, 1985.

Orr, J. C., Epitalon, J.-M., and Gattuso, J.-P.: Comparison of ten packages that compute ocean carbonate chemistry, Biogeosciences, 12, 1483–1510, https://doi.org/10.5194/bg-12-1483-2015, 2015.

Oudot, C., Gerard, R., Morin, P.: Precise shipboard determination of dissolved oxygen (Winkler procedure) for productivity studies with commercial system. Limnology and Oceanography 33, 146e150, 1988.

Pecci, M., Sferlazzo, D., Anello, F., Becagli, S., Colella, S., Silvestri, L. D., Iorio, T. D., Meloni, D., Monteleone, F., Piacentino, S., Principato, E., and Sarra, A. D.: Large influence of the 2022-23 marine heatwave on the air-sea CO2 flux in the Central Mediterranean, https://doi.org/10.22541/essoar.173393985.55347710/v1, 11 December 2024.

Pierrot, D., Lewis, E., and Wallace, D. W. R.: MS Excel Program Developed for CO2 system calculations. https://cdiac.ess -drive.lbl.cov/ftp/co2sys/CO2SYS_calc_XLS_v2.1/, 2006.

Ravaioli, M., Bergami, C., Riminucci, F., Langone, L., Cardin, V., Di Sarra, A., Aracri, S., Bastianini, M., Bensi, M., Bergamasco, A., Bommarito, C., Borghini, M., Bortoluzzi, G., Bozzano, R., Cantoni, C., Chiggiato, J., Crisafi, E., D'Adamo, R., Durante, S., Fanara, C., Grilli, F., Lipizer, M., Marini, M., Miserocchi, S., Paschini, E., Penna, P., Pensieri, S., Pugnetti, A., Raicich, F., Schroeder, K., Siena, G., Specchiulli, A., Stanghellini, G., Vetrano, A., and Crise, A.: The RITMARE Italian Fixed-Point Observatory Network (IFON) for marine environmental monitoring: a case study, Journal of Operational Oceanography, 9, s202–s214, https://doi.org/10.1080/1755876x.2015.1114806, 2016.

Riebesell, U., Gattuso, J. P., Thingstad, T. F., & Middelburg, J. J.:. Arctic ocean acidification: pelagic ecosystem and biogeochemical responses during a mesocosm study. Biogeosciences, 10, 5619-5626, doi:10.5194/bg-10-5619-2013, 2013.

Robinson, A.R., Leslie, W.G., Theocharis, A., and Lascaratos, A.: Mediterranean Sea circulation. Encyclopedia of Ocean Sciences Academic Press, Harcourt Science & Technology, Harcourt Place, 32 Jamestown Road London NW1 7BY UK, pp. 1689–1705, 2001.

Roether, W. and Schlitzer, R.: Eastern Mediterranean deep water renewal on the basis of chlorofluoromethane and tritium data, Dynamics of Atmospheres and Oceans, 15, 333–354, https://doi.org/10.1016/0377-0265(91)90025-b, 1991.

**ha formattato:** Colore carattere: Rosso

**ha formattato:** Colore carattere: Rosso

Schlitzer, R., Roether, W., Oster, H., Junghans, H.-G., Hausmann, M., Johannsen, H., and Michelato, A.: Chlorofluoromethane and oxygen in the Eastern Mediterranean, Deep Sea Research Part A. Oceanographic Research Papers, 38, 1531–1551, https://doi.org/10.1016/0198-0149(91)90088-w, 1991.

Schneider, A., Tanhua, T., Körtzinger, A., and Wallace, D. W. R.: High anthropogenic carbon content in the eastern Mediterranean, J. Geophys. Res., 115, https://doi.org/10.1029/2010jc006171, 2010.

Schroeder, K., Ben Ismail, S., Bensi, M., Bosse, A., Chiggiato, J., Civitarese, G., Falcieri M, F., Fusco, G., Gačić, M., Gertman, I., Kubin, E., Malanotte-Rizzoli, P., Martellucci, R., Menna, M., Ozer, T., Taupier-Letage, I., Vargas-Yáñez, M., Velaoras, D., and Vilibić, I.: A consensus-based, revised and comprehensive catalogue for Mediterranean water masses acronyms. Mediterranean Marine Science, 25(3), 783–791. https://doi.org/10.12681/mms.38736, 2024.

Steinhoff, T., Gkritzalis, T., Jones, S., Macovei, V. A., Neill, C., Schuster, U., Akl, J., Arruda, R., Atamanchuk, D., Barry, M., Beaumont, L., Cantoni, C., Dickson, A., Fahning, J., Fought, J., Frangoulis, C., Gutiérrez-Loza, L., Hagan, C., Honkanen, M., Kielosto, S., Kinski, N., Körtzinger, A., Landschützer, P., Lauvset, S. K., Lawrence-Slavas, N., Li, Q., Luchetta, A., Malarde, D., Paulsen, M., Ritschel, M., Rutgersson, A., Sanders, R., Shitashima, K., Spaulding, R., Stamataki, N., Stenbäck, K., Sutton, A., Tatkiewicz, W., Telszewski, M., Theetaert, H., Tilbrook, B., and Wanninkhof, R.: The ICOS OTC $pCO_2$ instrument intercomparison, Limnology & Ocean Methods, lom3.10727, https://doi.org/10.1002/lom3.10727, 2025.

Taillandier, V., D'Ortenzio, F., Prieur, L., Conan, P., Coppola, L., Cornec M., Dumas F., Durrieu de Madron X. , Fach B., Fourrier M., Gentil M., Hayes D., Husrevoglu S., Legoff H., Le Ster1 L., Örek H., Ozer T., Poulain P. M., Pujo-Pay M., Ribera d'Alcalà M., Salihoglu B., Testor P., Velaoras D., Wagener T., and Wimart-Rousseauet C.: Sources of the Levantine intermediate water in winter 2019. Journal of Geophysical Research: Oceans, 127, https://doi.org/10.1029/2021JC017506, 2022.

Takahashi, T., Olafsson, J., Goddard, J. G., Chipman, D. W., and Sutherland, S. C.: Seasonal variation of $CO_2$ and nutrients in the high-latitude surface oceans: A comparative study, Global Biogeochemical Cycles, 7, 843–878, https://doi.org/10.1029/93GB02263, 1993.

Takahashi, T., Sutherland, S. C., Wanninkhof, R., Sweeney, C., Feely, R. A., Chipman, D. W., Hales, B., Friederich, G., Chavez, F., Sabine, C., Watson, A., Bakker, D. C. E., Schuster, U., Metzl, N., Yoshikawa-Inoue, H., Ishii, M., Midorikawa, T., Nojiri, Y., Körtzinger, A., Steinhoff, T., Hoppema, M., Olafsson, J., Arnarson, T. S., Tilbrook, B., Johannessen, T., Olsen, A., Bellerby, R., Wong, C. S., Delille, B., Bates, N. R., and De Baar, H. J. W.: Climatological mean and decadal change in surface ocean pCO2, and net sea–air CO2 flux over the global oceans, Deep Sea Research Part II: Topical Studies in Oceanography, 56, 554–577, https://doi.org/10.1016/j.dsr2.2008.12.009, 2009.

The MathWorks Inc. MATLAB version: 9.13.0 (R2023b), Natick, Massachusetts: The MathWorks Inc. https://www.mathworks.com, 2022.

599 Touratier, F. and Goyet, C.: Impact of the Eastern Mediterranean Transient on the distribution of anthropogenic
600 CO2 and first estimate of acidification for the Mediterranean Sea, Deep Sea Research Part I: Oceanographic
601 Research Papers, 58, 1–15, https://doi.org/10.1016/j.dsr.2010.10.002, 2011.

602 Turk, D., Malačič, V., DeGrandpre, M. D., and McGillis, W. R.: Carbon dioxide variability and air-sea fluxes in
603 the northern Adriatic Sea, J. Geophys. Res., 115, 2009JC006034, https://doi.org/10.1029/2009JC006034, 2010.

604 Ulses, C., Estournel, C., Marsaleix, P., Soetaert, K., Fourrier, M., Coppola, L., Lefèvre, D., Touratier, F., Goyet,
605 C., Guglielmi, V., Kessouri, F., Testor, P., and Durrieu De Madron, X.: Seasonal dynamics and annual budget of
606 dissolved inorganic carbon in the northwestern Mediterranean deep-convection region, Biogeosciences, 20, 4683–
607 4710, https://doi.org/10.5194/bg-20-4683-2023, 2023.

608 Urbini, L., Ingrosso, G., Djakovac, T., Piacentino, S., and Giani, M.: Temporal and Spatial Variability of the CO2
609 System in a Riverine Influenced Area of the Mediterranean Sea, the Northern Adriatic, Front. Mar. Sci., 7,
610 https://doi.org/10.3389/fmars.2020.00679, 2020.

611 Urdiales-Flores, D., Zittis, G., Hadjinicolaou, P., Osipov, S., Klingmüller, K., Mihalopoulos, N., Kanakidou, M.,
612 Economou, T., and Lelieveld, J.: Drivers of accelerated warming in Mediterranean climate-type regions, npj Clim
613 Atmos Sci, 6, 97, https://doi.org/10.1038/s41612-023-00423-1, 2023.

614 Vilibić, I. and Orlić, M.: Least-squares tracer analysis of water masses in the South Adriatic (1967–1990), Deep
615 Sea Research Part I: Oceanographic Research Papers, 48, 2297–2330, https://doi.org/10.1016/s0967-
616 0637(01)00014-0, 2001.

617 Zittis, G., Hadjinicolaou, P., Klangidou, M., Proestos, Y., and Lelieveld, J.: A multi-model, multi-scenario, and
618 multi-domain analysis of regional climate projections for the Mediterranean, Reg Environ Change, 19, 2621–
619 2635, https://doi.org/10.1007/s10113-019-01565-w, 2019.

620

**ha formattato:** Colore carattere: Rosso

**ha formattato:** Colore carattere: Rosso

**ha formattato:** Colore carattere: Rosso